Similar Thrust Performance in Diverging-Magnetic-Field Electrostatic Thruster with Monoatomic Propellants

Daisuke Ichihara,[1] and Akihiro Sasoh[2]
Nagoya University, Nagoya, 464-8603, Japan

Nomenclature

e = elemental charge, C

F = thrust, N

J_d = discharge current, A

J_i = ion beam current, A

$\hat{J}_i \equiv J_i/(e\dot{m}/m)=$ normalized ion beam current

J_k = keeper current, A

$\dot{m} \equiv \dot{m}_a + \dot{m}_c$ = total flow rate, Aeq

$\dot{m}_a$ = propellant flow rate through the slit on the anode, Aeq

$\dot{m}_c$ = working gas flow rate of the cathode, Aeq

m = atomic mass, kg

r, z = cylindrical coordinates

u_{cr} = critical ionization velocity, m/s

$u_{ex} \equiv F/\dot{m}$ = mass-averaged exhaust velocity, m/s

V_d = discharge voltage, V

V_k = keeper voltage, V

ε = normalized specific input-energy

$<\varphi>$ = ion beam divergence half-angle, deg.

ϕ_i = ionization energy, eV

η = thrust efficiency

---

[1] Research associate, Department of Aerospace Engineering.
[2] Professor, Department of Aerospace Engineering, Associate Fellow AIAA.

I. Introduction

Among the noble gases, xenon (Xe) has been most widely used as the propellant for electric space propulsion primarily because of the favorable trade-off between availability, atomic mass, ionization energy, and ionization cross-section [1]. However, the excessive usage of xenon is almost prohibitively expensive compared to other viable alternatives. Currently, xenon costs $1440/kg, which is 240 times higher than the cost of argon [2]. In order to reduce the thruster operation cost, cheaper propellants are required. This is relevant to electrostatic thrusters, such as ion thrusters and Hall thrusters in particular since alternative propellants are actively being investigated in these two instances [3]. Linnell et al. [4] operated Hall thrusters with krypton and obtained a lower thrust efficiency than that of xenon, primarily because of its higher ionization cost. Shabshelowitz et al. [5] developed a helicon Hall thruster which used a helicon plasma source to enhance pre-ionization, and operated it with xenon, argon, and nitrogen. However, the increment in thrust performance did not compensate for the cost of the ion source power. Fujita et al. [6] successfully operated Hall thrusters with argon, and reported that the thrust efficiency was still lower than the value for xenon because about 50% of the propellant introduced in the acceleration region was not ionized. Although argon and krypton have the potential to lower the operation cost in electric space propulsion, many challenges still remain in regard to improving the thrust efficiency. Ichihara et al. [7] developed the diverging magnetic field electrostatic thruster (DM-EST), which comprised a diverging magnetic field between a ring anode that was coaxially set on the center axis, and a hollow cathode set at a cusp of the applied magnetic field. The thruster utilized the basic structure of a helicon electrostatic thruster [8].We developed the “near-anode ionization scheme” [9] in which the propellant was injected through an annular slit on the inner surface of a ring anode, so that efficient ionization and ion acceleration from the near anode to cathode potential were realized. In this report, we present the results for a newly developed DM-EST in which only permanent magnets and yokes are used to apply an external magnetic field, and examined its thrust performance by using the monoatomic species, argon, krypton, and xenon.

II. Experimental Apparatus and Methods

A. Diverging Magnetic Field Electrostatic Thruster

Figure 1 schematically illustrates the thruster head of the DM-EST developed in this study. The thruster shares common features with the thruster of Ref. [7]; they have a ring anode on the center axis, and an off-axis hollow cathode set in a cusp of the applied magnetic field in the downstream.

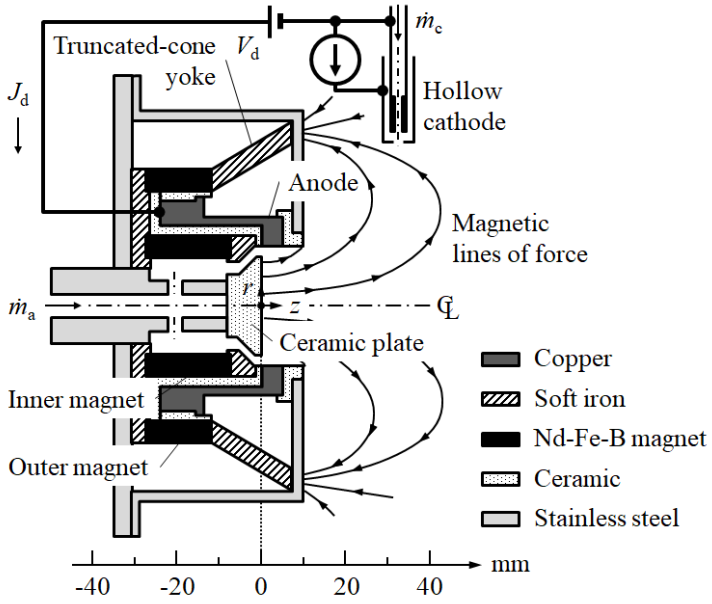

Fig. 1. Schematic of diverging magnetic field electrostatic thruster.

The ring anode is made of copper, with an inner diameter of 27 mm and a length of 5 mm. Inside the anode, a ceramic plate made of boron nitride plugs the passage of the propellant, except for the 1.5-mm-wide annular slit along the inner surface of the ring anode. The diverging magnetic field was applied using two ring Nd-Fe-B permanent magnets and soft-iron yokes. The inner magnet was used to strengthen the magnetic field on the inner surface of the anode to enhance the near-anode ionization [9]. This magnet has an inner diameter of 23 mm, an outer diameter of 33 mm, and a length of 20 mm. The outer magnet has an inner diameter of 55 mm, an outer diameter of 65 mm, and length of 15 mm. The applied magnetic field is greatly modified by the truncated-cone yoke to extend the diverging portion, which is followed by a field-free region in the cusp. The cylindrical coordinates (z, r) where z and r are the axial and radial coordinate, respectively, are defined in the axisymmetric configuration with their origin at the center of the downstream surface of the ceramic plate. The magnetic field strength was 75 mT at (z, r) = (0 mm, 0 mm) and 250 mT at (z, r) = (0 mm, 13.5 mm), respectively. The orifice

of a hollow cathode (DLHC-1000, Kaufman & Robinson, Inc.) was located at (z, r) = (32 mm, 37 mm) and the magnetic field strength was 5.8 mT at this point.

B. Thrust and Ion Beam Properties Measurement

A pendulum-type thrust stand with a 300-mm-long stand arm supported by two-knife-edge fulcrum was used to measure the thrust. The knife-edge is made of stainless steel 316 (iso number: X5CrNiMo17-12-2), and had a width of 10 mm and an apex angle of 90°. Each knife edge was mounted on a V-shaped groove with an opening angle of 120°. Each groove was formed by two blocks made of stainless steel 316 so that the bottom was not rounded. The displacement of the pendulum was measured by a laser displacement sensor (IL-S025, Keyence Co.) at the tip of the aluminum extension arm, where the distance from the fulcrum is 128 mm. The sensitivity of the thrust stand was calibrated in the range of up to 54 mN using a pulley and weight arrangement driven by a direct-current (DC) motor at the same ambient pressure as during the thruster operations. The calibrated conversion factor is 174 ± 0.33 mN/V. The thrust measurement uncertainty was 2.7% of the minimum thrust value measured in this study. A "tare force," is an apparent thrust that should be corrected in the thruster measurement. As described in Ref. [10], the tare force was measured beforehand. The tare force measurement uncertainty was 0.013 mN/A, which was 0.3% of the minimum thrust value measured in this study.

The same nude Faraday probe and its measuring circuit as in the previous work [9] were used to measure J_i and $\langle\phi\rangle$. The fulcrum of the 375-mm-long swing arm was at (z, r) = (9.5 mm, 0 mm). The definitions of J_i and $\langle\phi\rangle$ are also described in Ref. [9].

III. Experimental Results and Discussions

A. Operating Conditions

Table 1 summarizes the investigated operating conditions. Gas purity was 99.9999% for Ar, and 99.995% for Kr and Xe. The uncertainties in $\dot{m}_a$, V_d, and J_d were ± 3.0×10^{-2} Aeq, ± 2.0 V, and ± 51 mA, respectively. All experiments were conducted in a 1.2-m.dia., 3.0-m-long, stainless steel vacuum chamber. The maximum background pressure was 18 mPa at $\dot{m}_a$ = 3.0 Aeq, $\dot{m}_c$ = 0.36 Aeq of argon. Each operating condition was repeated at least three times while measuring F, J_d, J_i, $\langle\varphi\rangle$, and V_k. In the following figures, a symbol shows an

averaged value of each operating condition. The error bars in u_{ex} and J_d/J_i represent the standard deviation ($\pm\sigma$) obtained after a number of trials, while the error bars in $\hat{J}_i$ and $<\varphi>$ correspond to the uncertainty in the averaging.

Table 1 Operating conditions

Symbol	Unit	Setting		
-	-	Ar	Kr	Xe
m	Kg	6.6×10^{-26}	1.4×10^{-25}	2.2×10^{-25}
ϕ_i	eV	15.8	13.9	12.1
u_{cr}	km/s	8.7	5.6	4.2
$\dot{m}_a$	Aeq	2.0, 3.0	2.0	1.0
	mg/s	0.8, 1.2	1.7	1.3
$\dot{m}_c$	Aeq	0.36	0.36	0.36
	mg/s	0.15	0.31	0.48
$\dot{m}$	Aeq	2.36, 3.36	2.36	1.36
	mg/s	0.95, 1.35	2.01	1.78
V_d	V	150-350	200-300	175-250
J_k	A	2.0	2.0	2.0

B. Operation with argon

With the motivation described in the Introduction, this study highlights the thrust performance using argon which is shown in Fig. 2 . More than 150 V of V_d was necessary to breakdown and for steady-state operation. $\hat{J}_i$ gradually increased with increasing V_d. For only singly ionized particles, the value of $\hat{J}_i$ is equal to the propellant utilization efficiency. $\hat{J}_i$ becomes larger with $\dot{m}_a$ = 3.0 Aeq than with $\dot{m}_a$ = 2.0 Aeq, reflecting a higher electron-impact ionization rate with increasing $\dot{m}_a$.

As seen in Fig. 2, J_d/J_i remained at a constant of about 2.0 as V_d was varied. However, there is no clear difference between $\dot{m}_a$ = 2.0 Aeq and 3.0 Aeq.

u_{ex} increased with increasing V_d but was higher with $\dot{m}_a$ = 3.0 Aeq than with $\dot{m}_a$ = 2.0 Aeq. This suggests that with the higher flow rate, the ionization rate was increased so that the propellant was ionized upstream. In DM-EST operation, the electrical potential monotonically decreases towards downstream [9], ions which are generated closer to the anode will experience a larger potential drop for electrostatic acceleration.

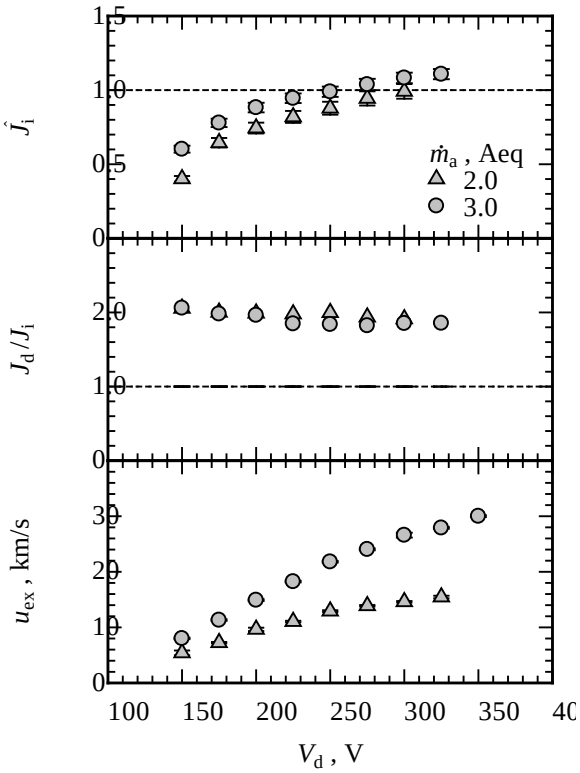

Fig. 2. $\hat{J}_i$, J_d/J_i and u_{ex} as a function of V_d with Ar.

C. Similarities in Thrust Performance

In this section, thruster performances with different propellant species are evaluated and characterized by using a normalized value. η is calculated as follows,

$$\eta \equiv \frac{F^2}{2\dot{m}\left(J_d V_d + J_k V_k\right)}. \tag{1}$$

Let a normalized parameter, ε, be defined as

$$\varepsilon \equiv \frac{\left(J_d V_d + J_k V_k\right)/\dot{m}}{e\phi_i/m}. \tag{2}$$

The numerator $(J_dV_d+J_kV_k)/\dot{m}$ and the denominator $e\phi_i/m$ represent specific input-energy and specific ionization-energy, respectively. Hence, ε represents the ratio of input-energy per particle to its the ionization energy. Figure 3 summaries the thruster performance parameters which are obtained with all the tested species as a function of ε. A symbol shows an average value and an error bar represents the uncertainty that is estimated by applying the law of propagation of errors to Eqs (1) and (2). Overall the operation characteristics among these

species have similarities with respect to ε. η increased with increasing ε with $\varepsilon \lesssim 30$, then was gradually saturated at 20% - 25%. The values of η for the different species are close to each other. For example, at $\varepsilon \approx 55$, η equals 23%, 25%, and 20% for Ar, Kr, and Xe, respectively. From Fig. 2, $\hat{J}_i$ evaluated for singly ionized plasma reached 1.0 at V_d = 250 V, which corresponds to ε = 30 with $\dot{m}_a$ = 3.0 Aeq. If the propellant injected from the slit is fully ionized (or supplying more than 30 of ε), η is expected to reach a comparable level even with Ar.

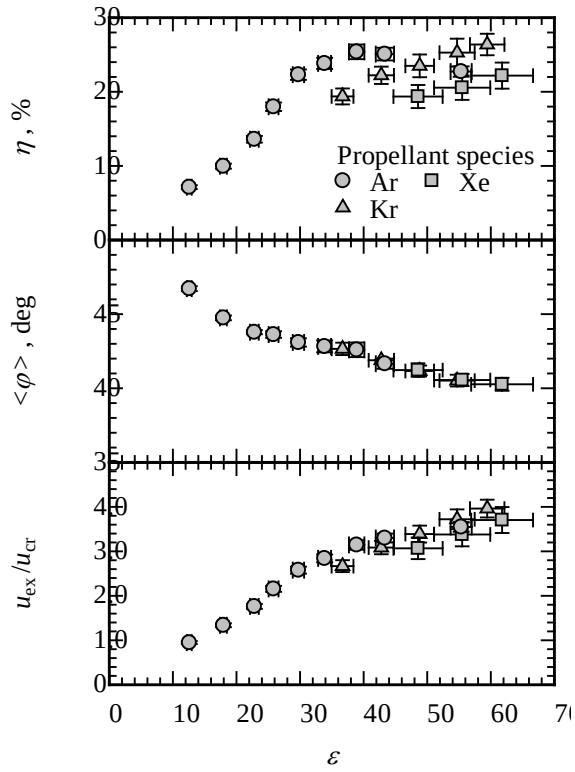

Fig. 3. η, <φ>, and u_{ex}/u_{cr} as a function of ε with Ar, Kr, and Xe.

As seen in Fig. 3, <φ> also has a similarity among the different species. With increasing ε, <φ> decreased and is gradually saturated at about 40 deg. Because electrostatic acceleration is a collision-less process, the ion trajectory depends only on the electric field configuration. Hence, being independent of the propellant species suggests that the ionization occurs in the same region with a similar electric field distribution so that the ions experience the same potential drop towards downstream.

Figure 3 also shows u_{ex}/u_{cr} as a function of ε. u_{ex}/u_{cr} also exhibits a similarity among the species. i.e., it increased with increasing ε. For example, at $\varepsilon \approx 55$, u_{ex}/u_{cr} = 3.5, 3.7, and 3.4 which correspond to 3100 s, 2100

s, and 1400 s of specific impulse for Ar, Kr, and Xe operation, respectively. In previous studies that attempted to electrostatically accelerate Ar propellant using Hall thrusters [5, 6], specific impulse were no more than 2000 s with less than 30% thrust efficiency. With respect to these performances, DM-EST has a better capability to extend even to a higher exhaust velocity range which has not been achieved with Kr or Xe, with a competitive thrust efficiency.

IV. Conclusion

We have experimentally demonstrated similar thrust performances for Ar, Kr, and Xe propellants in a newly-developed, permanent magnet DM-EST, in which the applied magnetic field has the diverging section for ion acceleration, that is followed by the field free section to neutralize the propellant. The thrust performance has similarities with respect to the normalized specific input-energy, ε. With $\varepsilon \lesssim 30$ the propellants injected through the annular slit was almost fully ionized, and all the propellant species yielded thrust efficiencies ranging from 20% to 25% with an exhaust velocity 3-4 times higher than the corresponding critical ionization velocity. These results emphasize the importance of utilizing argon to improve the availability of electric propulsion technology.

Acknowledgments

This study was supported by JSPS KAKENHI Grant No. 18H03813. The authors thank A. Saito, Y. Nakanishi, S. Goto, Y. Adachi, and R. Yamamoto at the Technical Division, Nagoya University for their valuable technical assistance. Various and enlightening discussions with Dr. Akira Iwakawa (Nagoya University) are also acknowledged.

References

[1] Sorokin, A. A., Shmaenok, L. A., and Bobashev, S. V., “Measurements of Electron-Impact Ionization Cross Sections of Argon, Krypton, and Xenon by Comparison with Photoionization,” *Physical Review A*, Vol. 61, No. 2, 2000, Paper 022723

doi: 10.1103/PhysRevA.61.022723

[2] Kieckhafer, A., and King, L. B., "Energetics of Propellant Options for High-Power Hall Thrusters," *Journal of Propulsion and Power*, Vol. 23, No. 1, 2007, pp. 21-26.
doi: 10.2514/1.16376

[3] Mazouffre, S., "Electric Propulsion for Satellites and Spacecraft: Established Technologies and Novel Approaches," *Plasma Source Science and Technology*, Vol. 25, No. 3, 2016, Paper 033002.
doi:10.1088/0963-0252/25/3/033002

[4] Linnell, J. A., and Gallimore, A. D., "Efficiency Analysis of a Hall Thruster Operating with Krypton and Xenon," *Journal of Propulsion and Power*, Vol. 22, No. 6, 2006, pp. 1402-1412.
doi: 10.2514/1.19613

[5] Shabshelowitz, A., Gallimore, A. D., and Peterson, P. Y., "Performance of a Helicon Hall Thruster Operating with Xenon, Argon, and Nitrogen," *Journal of Propulsion and Power*, Vol. 30, No. 3, 2014, pp. 664-671.
doi: 10.2514/1.B35041

[6] Fujita, D., Kawashima, R., Ito, Y., Akagi, S., Suzuki, J., Schönherr, T., Koizumi, H., and Komurasaki, K., "Operating Parameters and Oscillation Characteristics of an Anode-Layer Hall Thruster with Argon Propellant," *Vacuum*, Vol. 110, 2014, pp. 159-164.
doi: 10.1016/j.vacuum.2014.07.022

[7] Ichihara, D., Uchigashima, A., Iwakawa, A., and Sasoh, A., "Electrostatic Ion Acceleration Across a Diverging Magnetic Field," *Applied Physics Letters*, Vol. 109, 2016, Paper 053901.
doi: 10.1063/1.4960363

[8] Harada, S., Baba, T., Uchigashima, A., Yokota, S., Iwakawa, A., Sasoh, A., Yamazaki, T., and Shimizu, H., "Electrostatic Acceleration of Helicon Plasma using a Cusped Magnetic Field," *Applied Physics Letters*, Vol. 105, 2014, Paper 194101.
doi: 10.1063/1.4900423

[9] Ichihara, D., Iwakawa, A., and Sasoh, A., "Effects of Magnetic Field Profile near Anode on Ion Acceleration Characteristics of a Diverging Magnetic Field Electrostatic Thruster," *Journal of Applied Physics*, Vol. 122, 2017, Paper 043302.
doi: 10.1063/1.4995286

[10] Ichihara, D., Uno, T., Hisashi, K., Jaehun, J., Akira, I., and Sasoh, A., “Ten-Ampere-Level, Applied-Field-Dominant Operation in Magnetoplasmadynamic Thrusters,” *Journal of Propulsion and Power*, Vol. 33, No. 2, 2017, pp. 360-369.
doi: 10.2514/1.B36179